Semiconductors, 2024, Vol. 58, No. 1

Effect of proton and electron irradiation on the parameters of gallium nitride Schottky diodes

© A.A. Lebedev[1], A.V. Sakharov[1], V.V. Kozlovski[2], D.A. Malevsky[1], A.E. Nikolaev[1], M.E. Levinshtein[1]

[1] Ioffe Institute,
194021 St. Petersburg, Russia
[2] Peter the Great Saint-Petersburg Polytechnic University,
195251 St. Petersburg, Russia
E-mail: Shura.Lebe@mail.ioffe.ru

Received January 30, 2024
Revised February 5, 2024
Accepted February 29, 2024

The carrier removal rates during proton and electron irradiations of *n*-type GaN grown by metal-organic vapor phase epitaxy were determined. Irradiation was carried out with protons with energy of 15 MeV in the fluence range $0 \leq \Phi_p \leq 5 \cdot 10^{14}\,\mathrm{cm}^{-2}$; the range of fluences when irradiated with electrons with energy of 0.9 MeV was $0 \leq \Phi_n \leq 5 \leq 10^{16}\,\mathrm{cm}^{-2}$. The value of the removal rate during proton irradiation, $\eta_p \approx 140\,\mathrm{cm}^{-1}$, is close to the lower limit of currently known values of η_p and indicates a sufficiently high level of radiation resistance of the studied material with respect to proton irradiation. The rate of carrier removal under the influence of electron irradiation, η_e is $\approx 0.47\,\mathrm{cm}^{-1}$ and corresponds to the typical values of η_e for type gallium nitride obtained by various methods.

Keywords: gallium nitride, proton irradiation, electron irradiation, carrier removal rate.

DOI: 10.61011/SC.2024.01.58121.5980

1. Introduction

Gallium nitride is currently considered to be one of the most promising wide-band materials of semiconductor electronics. A large band gap $E_g = 3.4\,\mathrm{eV}$ and breakdown field strength $E_i \sim 3\,\mathrm{MV/cm}$, which is an order of magnitude higher than the E_i value in silicon ($\sim 0.3\,\mathrm{MV/cm}$), provide an opportunity to design GaN Schottky barrier diodes (SBDs) with blocking voltage U_b in excess of 1 kV and a near-unity ideality factor η [1–3].

The band gap of GaN is only slightly greater than E_g 4*H*-SiC (3.34 eV), which has already found wide application (see, e. g., [4]). However, GaN has several important potential advantages over silicon carbide: a higher electron mobility; a direct band gap, which allows one to construct efficient optoelectronic devices based on GaN; and the applicability of GaN/AlGaN heterostructures in devices with a two-dimensional electron gas with a high mobility.

The resistance of semiconductor devices to various types of irradiation (specifically, proton and electron irradiation) often dictates the feasibility and conditions of use of such devices in electronic systems of nuclear reactors, particle accelerators, and space and aviation electronics. The resistance of SiC-based devices to electron and proton irradiation was examined in a number of studies (see the corresponding references in [5,6]). It was found that one of the most important parameters (electron removal rate η_e) under electron irradiation may vary by more than 2 orders of magnitude (from 0.015 [7] to $1.67\,\mathrm{cm}^{-1}$ [8]) depending on the electron energy, the material fabrication method, and the doping nature and level. In the case of proton irradiation of SiC, carrier removal rate η_p falls within the range from ~ 10 [9] to $\sim 110\,\mathrm{cm}^{-1}$ [10].

The electron removal rate in the course of both electron and proton irradiation of *n*-type GaN also depends on the irradiation energy and dose, the fabrication method and the initial carrier concentration of GaN, and on the dislocation density in the irradiated material [11]. The values of η_e vary with these parameters, falling within the range from $\sim 10^{-1}$ to $10\,\mathrm{cm}^{-1}$ [12]. An increase in the carrier concentration in GaN SBDs subjected to proton irradiation was observed in [13]. As was noted in reviews [11,14], this effect may be indicative of the formation of shallow donor levels under irradiation and is possibly attributable to an insufficient purity of the initial epitaxial layers. In all the other cases, proton irradiation led to removal of electrons from the conduction band. The determined values of η_p range widely from 40 [15] to $10^4\,\mathrm{cm}^{-1}$ [16].

In the present study, the effect of irradiation with electrons with an energy of 0.9 MeV and protons with an energy of 15 MeV on the parameters of SBDs based on test GaN structures grown by metalorganic vapor-phase epitaxy is examined. Rates of carrier removal η_e and η_p from the base layers of the studied structures are determined.

2. Experimental conditions

The studied structures were grown by metalorganic vapor-phase epitaxy (MOVPE). on (0001) sapphire substrates 2 inches in diameter with the use of standard compounds in a Dragon 125 setup with a horizontal reactor with induction heating. A 2.4-μm-thick buffer layer of undoped GaN was grown first on a substrate, and layers doped heavily and weakly with silicon, each with a thickness of $\sim 1\,\mu$m, were grown after that. The concentration of electrons in these layers determined from capacitance-voltage measurements was $6 \cdot 10^{18}$ and $8 \cdot 10^{16}\,\text{cm}^{-3}$, respectively. The end stage of growth was *in situ* deposition of a thin passivating Si_3N_4 dielectric layer that suppressed leakage currents [17]. Nickel contacts $600\,\mu$m in diameter, which formed Schottky barriers, were fabricated by thermal deposition of Ni through a shadow mask.

Irradiation with protons with an energy of 15 MeV was performed in the pulsed mode at an MGTs-20 cyclotron. The repetition rate and the duration of pulses were 100 Hz and 2.5 ms, respectively. Irradiation with electrons with an energy of 0.9 MeV was performed in the pulsed mode with the repetition rate and the duration of pulses set to 490 Hz and $330\,\mu$s, respectively. Proton and electron irradiation was performed at room temperature. The temperature in these experiments was maintained with an accuracy of $\pm 5^\circ$C.

Isothermal current–voltage curves of diodes were measured at room temperature in the single-pulse mode. The pulse duration was $5\,\mu$s, and the repetition rate was 100 Hz.

3. Results and discussion

Figure 1 shows the forward current–voltage curves of the initial diode (curve *1*) and diodes irradiated with four doses of protons with an energy of 15 MeV at room temperature.

At all fluences Φ, current–voltage curves were measured within the following range of current densities: $5 \cdot 10^{-6} \le j \le 1\,\text{A/cm}^2$. As in the case of SiC Schottky diodes, irradiation has almost no effect on the current–voltage curves under biases U lower than cut-off voltage U_c (when almost the entire applied voltage falls on the Schottky barrier and dependence $I(U)$ is exponential; see, e.g., [6]).

At $U > U_c$, the differential base resistance of diodes increases monotonically with increasing fluence Φ. The variation of mobility under irradiation may be neglected at relatively low values of Φ [18]. The electron concentration is then proportional to the differential base resistance, and rate η_p of electron removal from the base under irradiation may be calculated as $\eta_p = (n_0 - n)/\Phi$, where n_0 is the electron concentration in the base in the initial sample and n is the concentration after irradiation with fluence Φ.

The inset in Figure 1 demonstrates that the carrier concentration decreases linearly with increasing fluence at relatively small values of Φ. The slope of dependence $n(\Phi)$ within this section corresponds to carrier removal rate $\eta_p \approx 140\,\text{cm}^{-1}$. With this $n(\Phi)$ dependence, condition $n = 0$ should be satisfied at $\Phi \approx 5.5 \cdot 10^{14}\,\text{cm}^{-2}$ (dashed line in the inset in Figure 1). However, the value of n at $\Phi = 5 \cdot 10^{14}\,\text{cm}^{-2}$ is significantly higher than the one corresponding to a linear $n(\Phi)$ dependence. According to the analysis reported in [19], this result may indicate that GaN differs from SiC in supporting the following compensation mechanism under proton irradiation: a radiation-induced defect (vacancy) interacts with a shallow impurity atom, forming an electrically neutral or acceptor center. This compensation mechanism is typical, for example, in the case of electron irradiation of Si.

Figure 2 shows the forward current–voltage curves of the initial diode (curve *1*) and diodes irradiated with three doses of electrons with an energy of 0.9 MeV at room temperature.

Current–voltage curves were measured within the $1 \cdot 10^{-8} \le j \le 1\,\text{A/cm}^2$ current density range. As in the case of proton irradiation, irradiation with electrons has almost no effect on current–voltage curves under biases $U < U_c$.

In the $0 \le \Phi \le 6 \cdot 10^{16}\,\text{cm}^{-2}$ region, the differential base resistance increases monotonically with increasing Φ. If

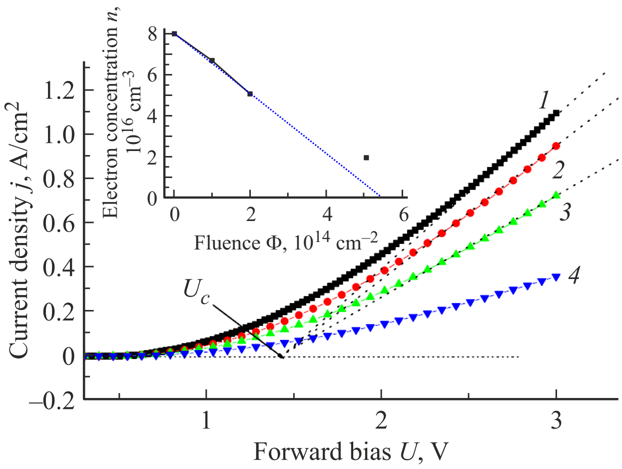

Figure 1. Forward current–voltage curves of diodes after irradiation with protons with an energy of 15 MeV at different fluences Φ, cm^{-2}: *1* — 0, *2* — $2 \cdot 10^{14}$, *3* — $4 \cdot 10^{14}$, and *4* — $5 \cdot 10^{14}$. The dependence of electron concentration in the diode base on fluence Φ in shown in the inset. (A color version of the figure is provided in the online version of the paper).

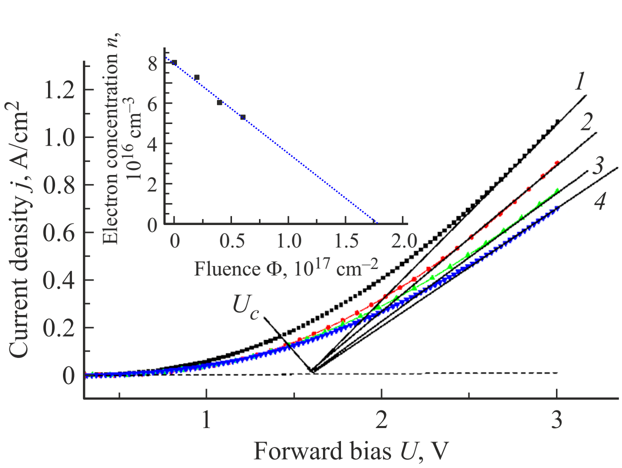

Figure 2. Forward current–voltage curves of diodes after irradiation with electrons with an energy of 0.9 MeV at different fluences Φ, cm^{-2}: *1* — 0, *2* — $2 \cdot 10^{16}$, *3* — $4 \cdot 10^{16}$, and *4* — $6 \cdot 10^{16}$. The dependence of carrier concentration in the diode base on fluence Φ in shown in the inset.

one follows the same approach as the one used for proton irradiation and neglects the change in mobility, it becomes easy to calculate the variation of electron concentration with fluence Φ (see the inset in Figure 2) based on the data from Figure 2. It is evident that the electron concentration decreases linearly with increasing fluence. The slope of dependence $n(\Phi)$ corresponds to electron removal rate $\eta_e \approx 0.47\,\text{cm}^{-1}$.

The determined value of $\eta_p \approx 140\,\text{cm}^{-1}$ is close to the lower boundary of the range of carrier removal rates under proton irradiation and indicates a sufficiently high level of radiation resistance. The $\eta_e \approx 0.47\,\text{cm}^{-1}$ value corresponds roughly to the center of the literature range of carrier removal rates under electron irradiation.

4. Conclusion

In conclusion, it should be noted that the value of $\eta_p \approx 140\,\text{cm}^{-1}$ determined for *n*-type GaN is close to the lower boundary of the range of carrier removal rates under proton irradiation and indicates a sufficiently high level of radiation resistance (specifically, a level comparable to the radiation resistance of *n*-type silicon carbide). The electron removal rate of $\eta_e \approx 0.47\,\text{cm}^{-1}$ determined in the study corresponds roughly to the center of the literature range of η_e values for *n*-type GaN. This value is also comparable to η_e levels typical of *n*-type SiC.

Funding

This study was supported in part by grant No. 22-12-00003 from the Russian Science Foundation.

Conflict of interest

The authors declare that they have no conflict of interest.

References

[1] X. Liu, P. Zou, H. Wang, Yu. Lin, J. Wu, Z. Chen, X. Wang, Sh. Huang. IEEE Trans. Electron Dev., **70**, 3748 (2023).
[2] M. Matys, K. Kitagawa, T. Narita, T. Uesugi, J. Suda, T. Kachi. Appl. Phys. Lett., **121**, 203507 (2022).
[3] D. Khachariya, Sh. Stein, W. Mecouch, M. Hayden Breckenridge, Sh. Rathkanthiwar, S. Mita, B. Moody[1], P. Reddy, J. Tweedie, R. Kirste, K. Sierakowski, G. Kamler, M. Bockowski, E. Kohn, S. Pavlidis, R. Collazo, Z. Sitar. Appl. Phys. Express, **15**, 101004 (2022).
[4] A.A. Lebedev, P.A. Ivanov, M.E. Levinshtein, E.N. Mokhov, S.S. Nagalyuk, A.N. Anisimov, P.G. Baranov. Phys.-Usp., **62** (8), 754 (2019).
[5] A.A. Lebedev, V.V. Kozlovski, M.E. Levinshtein, D.A. Malevsky, R.A. Kuzmin. Semiconductors, **56** (8), 594 (2022).
[6] A.A. Lebedev, V.V. Kozlovski, M.E. Levinshtein, D.A. Malevsky, G.A. Oganesyan. Semiconductors, **57** (1), 49 (2023).
[7] V.V. Kozlovski, A.A. Lebedev, E.V. Bogdanova. J. Appl. Phys., **117**, 155702 (2015).
[8] E. Omotoso, W.E. Meyer, F. D. Auret, A.T. Paradzah, M. Diale, S.M.M. Coelho, P.J. Janse, van Rensburg. Mater. Sci. Semicond. Process., **39**, 112 (2015).
[9] Z. Luo, T. Chen, J.D. Cressler, D.C. Sheridan, J.R. Williams, R.A. Reed, P.W. Marshall. IEEE Trans. Nucl. Sci., **50**, 1821 (2003).
[10] V. Emtsev, A. Ivanov, V. Kozlovski, A. Lebedev, G. Oganesyan, N. Strokan, G. Wagner. FTP, **46**, 473 (2012).
[11] S.J. Pearton, F. Ren, E. Patrick, M.E. Law, A.Y. Polyakov. ECS J. Solid State Sci. Tech., **5** (2), Q35 (2016).
[12] A.Y. Polyakov, In-Hwan Lee, N.B. Smirnov, A.V. Govorkov, E.A. Kozhukhova, N.G. Kolin, A.V. Korulin, V.M. Boiko, S.J. Pearton. J. Appl. Phys., **109**, 123703 (2011).
[13] S. Narita, T. Hitora, E. Yamaguchi, Y. Sakemi, M. Itoh, H. Yoshida, J. Kasagi, K. Neich. Nucl. Instrum. Meth. Phys. Res. A, **717**, 1 (2013).
[14] S.J. Pearton, R. Deist, F. Ren, Lu Liu, A.Y. Polyakov, J. Kim. J. Vac. Sci. Technol. A, **31** (5), 050801 (2013).
[15] M. Hayes, F.D. Auret, L. Wu, W.E. Meyer, J.M. Nel, M.J. Legodi. Physica B, **340**–**342**, 421 (2003).
[16] V.V. Emtsev, V.Yu. Davydov, E.E. Haller, A.A. Klochikhin, V.V. Kozlovskii, G.A. Oganesyan, D.S. Poloskin, N.M. Shmidt, V.A. Vekshin, A.S. Usikov. Physica B: Condens. Matter, **308**–**310**, 58 (2001).
[17] D. Zakheim, W. Lundin, A. Sakharov, E. Zavarin, P. Brunkov, E. Lundina, A. Tsatsulnikov, S. Karpov. Semicond. Sci. Technol., **33**, 115008 (2018).
[18] M.E. Levinshtein, S.L. Rumyantsev, M.S. Shur (eds). *Properties of Advanced Semiconductor Materials: GaN, AIN, InN, BN, SiC, SiGe* (John Wiley & Sons Inc., N.Y., 2001).
[19] A.A. Lebedev, V.V. Kozlovski, K.S. Davydovskaya, M.E. Levinshtein. Materials, **14**, 4976 (2021).

Translated by D.Safin